



Published in final edited form as:

Mod Pathol. 2016 April ; 29(4): 381–390. doi:10.1038/modpathol.2016.27.

Evidence for spleen dysfunction in malaria-HIV co-infection in a subset of pediatric patients

Regina Joice¹, Charles Frantzreb^{1,2}, Alana Pradham², Karl B. Seydel^{3,4}, Steve Kamiza⁵, Dyann F. Wirth¹, Manoj T. Duraisingh¹, Malcolm E Molyneux^{4,5,6}, Terrie E. Taylor^{3,4}, Matthias Marti¹, and Danny A. Milner Jr.^{1,2,3,*}

¹The Harvard School of Public Health, Boston, Massachusetts, USA

²The Brigham & Women's Hospital, Boston, Massachusetts, USA

³The Blantyre Malaria Project, University of Malawi College of Medicine, Blantyre, Malawi

⁴College of Osteopathic Medicine, Michigan State University, East Lansing, Michigan, USA

⁵University of Malawi, College of Medicine, Blantyre, Malawi

⁶Malawi-Liverpool-Wellcome Trust Clinical Research Programme, Blantyre, Malawi

⁷Liverpool School of Tropical Medicine, UK

Abstract

The spleen has an important role in the clearance of malaria parasites, and the role of HIV co-infection on this process is yet to be described. Using a combination of histological and molecular methods, we systematically evaluated parasite load across multiple organs from HIV-positive and HIV-negative cases of an autopsy study of pediatric comatose children with malaria infection (n = 103) in Blantyre, Malawi. Quantification of parasite load across organs was done using histology. A subset of cases was further characterized for parasite localization and stage of development using immunohistochemistry-based labeling of parasite and host cells (5 HIV-positive, 10 HIV-negative), and quantitative RT-PCR (qRT-PCR) of asexual and sexual-specific genes (4 HIV-positive, 5 HIV-negative). The results were compared with clinical information including HIV status. The HIV positive rate was 21% for the group studied (20 of 95) and HIV-positive patients had a significantly shorter duration of time between onset of illness and death, and were significantly older than HIV-negative patients. We found that spleens of HIV-positive cases had significantly higher parasite loads compared to those of HIV-negative cases in each the three methods we used: (i) standard histology, (ii) immunohistochemistry-based labeling of *Plasmodium lactate dehydrogenase* (pLDH), and (iii) molecular detection of asexual parasite transcript *apical*

Users may view, print, copy, and download text and data-mine the content in such documents, for the purposes of academic research, subject always to the full Conditions of use: http://www.nature.com/authors/editorial_policies/license.html#terms

Corresponding Author: Danny A. Milner, Jr, MD, MSc, FCAP, The Brigham and Women's Hospital, Department of Pathology, 75 Francis Street, Amory 3, Boston, Massachusetts 02115, ; Email: dmilner@partners.org, Office: 617-525-7761

Supplementary information is available at *Modern Pathology's* website

Disclosure/Conflict of Interest: None of the authors have any conflict of interests to report regarding this manuscript. This work was supported by the U.S. National Institutes of Health (DAM: RO1 AO34969, K23 AI072033, MM: R01A1077558, TT: 5R01AI034969-14, RJ: T32 AI007535), the Harvard Initiative for Global Health, Harvard Catalyst, and by The Wellcome Trust, U.K (042390/Z/94).

membrane antigen 1 (AMA1). Immunohistochemistry-based labeling of macrophage marker CD163 in a subset of spleens revealed fewer activated macrophages containing engulfed parasites and a greater number of free unphagocytosed parasites in the HIV-positive cases. The mechanism by which HIV infection is associated with more rapid progression to severe cerebral malaria disease is possibly impairment of parasite destruction by splenic macrophages, supported by published *in vitro* studies showing inefficient phagocytosis of malaria parasites by HIV-infected macrophages.

Keywords

Plasmodium falciparum; autopsy; spleen; HIV; macrophages; malaria

INTRODUCTION

Cerebral malaria (CM) is caused by the parasite *Plasmodium falciparum*, and in children is commonly associated with seizures and coma. Autopsies of cerebral malaria patients show increased brain volume and parasites sequestered within red cells in the cerebral microvasculature⁽¹⁾. Of patients meeting the clinical case definition of cerebral malaria, a secondary classification of CM1 or CM2 can be made based on the gross and histological findings in the brain⁽²⁾. The pathological features of CM1 are defined as having dense sequestration only, while for CM2 are defined as having in addition to cerebral sequestration, the presence of ring hemorrhages, excessive parasite pigment, and free pigment “ghosts”. For both of these classifications, more than 20% of vessels are parasitized at autopsy and there is no other cause of death identified. One possible hypothesis is that CM1 and CM2 represent different time points of cerebral malaria, i.e. CM1 cases are those in which death occurs during active sequestration while in CM2 death occurs after a duration which includes schizont rupture of sufficient magnitude to produce additional histopathology. An alternative hypothesis is that the underlying pathophysiology of the two phenotypic CM states is different. In the cohort presented here, ~60% of CM1 patients were HIV positive, suggesting a possible role of HIV on the CM1/CM2 distinction⁽³⁾.

The spleen is important in removing malaria parasites from the blood, and thereby controlling the infection, and yet the role of HIV co-infection in this process is yet to be described. The spleen as an organ of immune processing and filtration has the entire blood volume of a patient passed through its parenchyma numerous times per day. During a malaria infection, many early ring stage forms of *Plasmodium falciparum* within red blood cells likewise pass through the spleen and do so unencumbered. As parasites grow and alter the surface of the host red blood cell, the spleen and its surveillance cells identify infected cells and prevent them from further circulation. The spleen is capable of retaining late stage trophozoite stages (with dramatic surface modifications and increased host cell rigidity) as well as a fraction of earlier ring-stage parasites (with slight modifications and slightly altered deformability)⁽⁴⁾. These parasitized RBCs may be trapped and retained within the cords of the splenic red pulp^(4, 5), where they are then phagocytosed or pitted (removal of parasite leaving host cell intact) by resident macrophages⁽⁶⁾. The alterations of cell surface are the basis for *P. falciparum* sequestration in the microvasculature of other tissues (brain,

gut, etc)^(7, 8), a process that enables successfully sequestered parasites to avoid destruction as they pass through the spleen.

In our cohort, patients with active malaria infections, very high parasitemia, but not severe malaria (CM3) ⁽²⁾ had little or no parasites present in the spleen at autopsy less than 48 hours later. The presence of parasites in the spleen at autopsy may suggest that the malarial infection has overwhelmed the capacity of the spleen to clear parasites. The primary cell involved in this process is the macrophage, resident and circulating through the red pulp (the slow circulation of the spleen). If the ability of macrophages to phagocytose were disturbed, regardless of etiology, we could hypothesize that the spleen's capacity would be overwhelmed and high total body parasitemia would be achieved at a rapid rate. This has in fact been observed in splenectomized individuals who have a higher parasite burden in the peripheral blood and are at higher risk of morbidity and mortality from malaria, likely due to their inability to control their parasitemia ^(9, 10). Under this hypothesis, it would follow that some cases of cerebral malaria in which the spleen's capacity is overwhelmed may be associated with a higher parasite burden in the body, including the spleen and brain, resulting in the CM1 phenotype.

As HIV prevalence is high in many malaria endemic regions, many children diagnosed with severe malaria are also HIV-positive. The effect of malaria on HIV viral load is complex and variable⁽¹¹⁻¹⁵⁾. Some studies have shown no association with viral load and malaria status while others demonstrated increased malarial episodes as viral load increased. More conclusive evidence exists for CD4 count, as a number of studies have demonstrated that the HIV-associated drop in CD4 count correlates with increased density of parasites, increased number of malaria complications and increased case fatality rate in patients with severe malaria ⁽¹⁶⁻¹⁹⁾. Mechanistically, HIV has been shown to impair the development of opsonizing antibodies to variant surface antigens ⁽²⁰⁾, and *in vitro* experiments have demonstrated that HIV infection impairs phagocytosis of opsonized infected erythrocytes by macrophages⁽²¹⁾. Based on these observations, we chose to test the hypothesis that among children with fatal malaria, HIV-infected patients would have a higher burden of parasites in the spleen and body overall than those without HIV. Following on our alternative hypothesis of CM1 above, we postulate that HIV could be one underlying biological condition to at least partially explain the difference between the CM categorizations.

Here we examined a large series of autopsy cases to investigate the underlying histological differences between HIV-positive and HIV-negative individuals across CM categories. We found that HIV-positivity across CM categories in this autopsy series is associated with faster progression from first symptom to death and increased asexual parasite burden across multiple organs of the body. This trend was most striking and most significant in the spleen. Further, macrophage dysfunction was apparent in the spleens of HIV-positive individuals, in particular, those with the CM1 phenotype. These findings suggest that HIV infection may be a biological contributor to the different phenotypes of CM pathology observed in our cohort suggesting the underlying pathobiology of the two phenotypes may be different.

METHODS

Autopsy series

The autopsies analyzed in this study (n = 103) are part of a pediatric severe malaria and postmortem autopsy study that was performed between 1996 and 2011⁽²⁾. Children meeting the clinical case definition of CM, as well as non-CM controls were admitted to the Pediatric Research Ward in the Queen Elizabeth Central Hospital in Blantyre, Malawi and enrolled in the severe malaria study upon the consent of the parent or guardian. Criteria used for diagnosis and clinical management have been previously described⁽²⁾. Autopsies were performed between 2 and 14 hours after death. Tissue specimens were collected in 10% buffered formalin or frozen immediately to be later used for histological examination, immunohistochemistry analysis, and qRT-PCR.

The institutional review boards (IRB) at the University of Malawi College of Medicine, Michigan State University, and the Harvard School of Public Health approved all aspects of the study. Written informed consent was obtained from all parents/guardians of the enrolled patients. IRB at the Brigham and Women's Hospital approved parts of this study including the use of discarded surgical tissue for laboratory optimization experiments.

Histology

Sections of brain, lung, heart, stomach, jejunum, ileum, colon, spleen, and skin were counted for number of parasites per 10 high powered field (hpf) as previously described^(2, 22, 23).

Sections of spleen stained with Hematoxylin and eosin were photographed at 200× with a polarizing lens. Briefly, three random 200× fields were photographed under ultra bright conditions (Light intensity = 6; Exposure = 106 ms) using a digital microscope camera (Q Color 3, Olympus America, Inc.). Within ImageJ (imagej.nih.gov/ij/), each image was split into three channels and the red channel was analyzed because the pigment, under the above conditions, transmits primarily red light. An automated macro within ImageJ was written which performed the following functions for each image: a) set a standard threshold for each image, b) partitioned an area of the field, c) analyzed particles for size and area, d) repeated b & c 9 times for a total of 10 different partitions (with overlap)⁽²⁴⁾. The thirty measurements (i.e., 3 images × 10 partitions/image) for size of particles and area occupied by particles of each case were averaged and a standard deviation was calculated. All measurements and calculations were carried out blinded to the final diagnosis.

Depigmented, Giemsa stained slides were produced as follows: Unstained slides were placed in saturated alcoholic picric acid (Poly Scientific) and covered with parafilm or other airtight means for 48 hours. The slides were rinsed in 90% then 70% alcohol, washed in running tap water until the yellow color disappeared, and then stained with a Giemsa for parasites⁽²⁵⁾. Slides were then photographed without a polarizing lens at 1000× under oil immersion. Three images were taken in the red pulp of the spleen, as well as areas of red pulp adjacent to white pulp. The number of parasites present in each slide was counted using ImageJ Cellcounter. In images taken from the border of the red and white pulp, separate counts were taken for macrophages, parasites phagocytized by macrophages, and parasites outside of macrophages; no macrophages were observed in the middle of the red pulp.

Autopsy tissues used for Immunohistochemistry and qRT-PCR

We performed our immunohistochemistry (IHC) analysis on 15 of the most recent cases for which there was a formalin-fixed paraffin embedded (FFPE) tissue sample archived from all nine sites of interest (spleen, heart, brain, lung, liver, bone marrow, gut, kidney, and subcutaneous fat). Tissue quality assessments were previously described in a study focused on gametocyte enrichment in the same cohort⁽²⁶⁾. In that study, we started with the 13 most recent HIV-negative cases for which all 9 tissue types were available. We assessed tissue quality by performing IHC using the platelet endothelial cell adhesion molecule 1 (PECAM-1 or CD31) to label endothelial cells on three tissue types: spleen, heart and bone marrow. For cases in which CD31 failed in at least one of the three tissues, we excluded those cases. The 10 most recently collected HIV-negative cases that met quality control criteria were used for a full organ screen using pLDH and Pfs16 and data from these are previously published⁽²⁶⁾. In the present study, we compare those published data to the 5 most recent HIV cases that satisfied the same criteria (all tissue types archived in FFPE, CD31-positivity in spleen, heart and bone marrow) and collected in the same years as the previously published HIV-negative cases.

For the qRT-PCR, we analyzed RNA from a smaller subset of patients for which all tissue samples were stored in RNAlater. Since this was not done at the start of the autopsy study, only 12 total cases had this sample type available. In the previous study⁽²⁶⁾, we performed RNA quality assessments. One case was determined to have poor RNA quality as determined by lack of clear RNA bands on the Agilent Bioanalyzer. After excluding patients for which not all tissues were available or poor RNA bands, there were 4 HIV-positive and 5 HIV-negative cases.

Immunohistochemistry (IHC)

Formalin-fixed paraffin-embedded tissues and control blocks were cut into 3 micron sections and mounted on slides. IHC for host markers CD163 and CD8 was performed as described previously^(26, 27). For parasite antigens, sections were dried overnight at 37°C, deparaffinized in xylene, and hydrated through a series of graded alcohols, finishing in water. Antigen retrieval was performed by incubating slides at approximately 95°C in a steamer for 20 minutes in an EDTA solution (1 mM EDTA + 0.05% Tween at pH 8). Slides were blocked using a universal blocking buffer (Thermo Scientific) for 20 minutes, followed by 10 minutes each of avidin and biotin blocking steps to block endogenous biotin and avidin, respectively. Parasite labeling was done as performed previously^(26, 28). Briefly, antibody incubation was then performed for 1 hour with a mouse monoclonal antibody against *Plasmodium* lactate dehydrogenase (pLDH; Dr. Michael Makler, FlowInc, Portland, OR) diluted 1:750 in blocking buffer, or with a mouse polyclonal anti-Pfs16 antibody (Dr. Kim Williamson, Loyola University, Chicago, IL), diluted 1:5000. Secondary anti-mouse biotinylated antibodies were used, followed by streptavidin conjugated to alkaline phosphatase (AP). Wash steps, in between each step thereafter were performed with TBS + 5% Tween for 3 × 5 minutes. For the development of signal, naphthol phosphatase-fast red chromagen reagent was applied. Slides were subsequently rinsed in water and counterstained in Mayer's hematoxylin, and mounted in aqueous mounting medium. Slides were blinded to patient ID and independently counted by two microscopists, counting parasites in 100

consecutive high power fields, starting in the upper left corner of each section. The averages of the microscopists' counts were used for the analysis.

RNA Extraction, DNase Digest and Reverse Transcription

Small pieces of tissue were snap frozen and stored at -80°C in RNAlater in eppendorf tubes until processing. Tissue samples were processed as described previously⁽²⁶⁾. Briefly, all samples were homogenized and processed in TRI Reagent BD (Molecular Research Center) per manufacturer instructions. RNA was cleaned up using DNase digest (Ambion) and an additional phenol-chloroform extraction for protein removal and sample concentration. First strand cDNA synthesis was performed using the SuperScript III First Strand Synthesis kit (Invitrogen). A total of 5000ug of RNA was input into cDNA synthesis reactions, and cDNA from 167 ug of RNA input went into each quantitative PCR reaction for those tissues for which 5000 ug of RNA could be isolated. For those samples for which less than 5000ug RNA was isolated, the total amount of RNA input was recorded and final calculations were adjusted to the total RNA input per reaction.

Quantitative RT-PCR

Quantitative PCR was performed on cDNA in 20 uL reaction volumes in either an ABI 7300 or ViiA7 machine (both, Applied Biosystems). Amplification was performed using iQ SYBR Green Master Mix (BioRad), and primers for stage-specific and housekeeping genes, published previously at 250nM concentration^(26, 29). Reaction conditions were as follows: 1 cycle \times 10 min at 95°C and 40 cycles \times 30 sec at 95°C and 1 min at 58°C . Each cDNA sample was run in triplicate, and each plate contained a dilution series of cDNA amplicons for each gene cloned into pGEM T-Easy plasmids (Promega). The genes included established markers with peak transcription during late asexual development: apical membrane antigen 1 (*AMA1*) and late gametocyte development (*Pfs25*), along with the constitutively expressed marker *ubiquitin conjugating enzyme* (*UCE*, *PF08_0085*), previously described⁽³⁰⁾. A 100-fold dilution series ranging from 5×10^1 to 5×10^9 was run on each plate and demonstrated that each primer pair was between 90–110% efficient and had a detection limit ranging between $10^1 - 10^2$ copies. The total number of transcript copies per RNA input of the sample was calculated using the CT values from a standard curve of plasmids with known concentration, and known size of plasmid and insert. The transcript copy number per sample was normalized to the total RNA input per PCR reaction. Relative expression of the stage-specific markers was calculated as a ratio of the transcript copy number of *AMA1* and *Pfs25*, respectively, compared to *UCE*.

Statistical Analysis

Clinical and demographic parameters were compared between HIV-positive and HIV-negative patients using either an ANOVA (parametric), Fisher's exact test (proportions) or Kruskal Wallace test non-parametric) between CM phenotype categories. Significant results are shown with p values reported. For histology, immunohistochemistry and quantitative PCR data, nonparametric tests were used to determine significant differences in parasite marker expression in HIV-positive and HIV-negative tissues. Mann-Whitney test with Bonferroni correction was used for comparisons of histology data. Mann-Whitney tests were used for comparisons of both IHC and qRT-PCR data. Significant findings are denoted in the

figures, tables and text, with p values reported. Throughout the paper, p-values less than 0.05 were considered significant.

RESULTS

Diverse clinical phenotypes are represented in cerebral malaria patients

Within the group of 103 autopsy cases of cerebral malaria used in this study, we captured a wide range of clinical phenotypes on these cases, including cases from across the range of CM categorizations. Cerebral malaria was represented by 13 CM1 and 40 CM2 patients. Other cases included those meeting the clinical case definition of cerebral malaria but dying of other non-CM causes (CM3, n=20) and Other (n = 22) patients who did not meet the clinical case definition (including parasitemic and aparasitemic patients). When stratifying the data by cerebral malaria phenotype, patients with CM1 compared to patients with CM2 had a shorter median duration between illness onset and death (34 hours vs 75 hours, $p = 0.0178$, Kruskal Wallance test), and also had higher medians of parasite density, hematocrit, platelet count, and a lower median blood lactate concentration, than CM2 individuals (Table S1). The HIV-positive rate was significantly higher for CM1 vs. CM2 (57% vs 18%, $p = 0.006$, Fisher's exact test) (Table S1).

HIV-positivity is associated with faster progression from admission to death

We examined 95 patients, of whom 20 were HIV + (21%), out of 103 autopsies (no HIV results were available for 8 patients) (Table 1). HIV-positive patients were older than HIV-negative patients (79 versus 26 median months of age, $p = 0.0023$, Mann Whitney U). Gender and other clinical measurements that relate to severe malaria such as density of blood parasitemia, hematocrit, blood lactate concentration, white blood cell count and platelet count showed no significant differences in means between the groups. However, the mean interval between onset of symptoms and death was significantly shorter in HIV-positive patients, who died around two days after onset of symptoms, as compared with over three days for HIV-negative patients (50 versus 78 hours, $p = 0.0084$, Mann Whitney U). Since this autopsy study took place between 1996 and 2010, at the time many of these patients were enrolled in the study, CD4 counts and HIV viral loads were not being routinely measured in Malawi and certainly not in acutely ill children. However, we obtained HIV viral load measurements for a subset of the HIV-positive cases in this study. This data comes from a parallel analysis focused on the brain pathology during malaria-HIV coinfection in this same autopsy cohort (³¹). In the Hochman et al paper, viral loads were retrospectively measured using archived plasma and clinical charts were evaluated to determine whether these individuals met the clinical case definition of AIDS, as according to the WHO guidelines for HIV severity. Of the 20 HIV-positive patients, 14 had plasma available for this analysis, and all 14 had quantifiable viral loads by quantitative PCR. In terms of AIDS, it was determined that all individuals had Stage 1/2 (mild disease) and stage 3/4 (severe disease), but none met the clinical case criteria for AIDS. Thus, differences in malaria disease severity and progression in this cohort appear largely due to HIV-infection during the mild and severe stages, but prior to the onset of AIDS. Notably, none of the children in this study were on anti-retroviral therapy.

Greater parasite burden in the spleens of HIV-positive individuals

To further explore the basis of this rapid progression from symptoms to death in the HIV-malaria co-infected group, we compared the parasite burden in multiple organs in the autopsy cases. There was a higher mean parasite load in multiple organs of HIV-positive cases compared to HIV-negative cases, with differences approaching statistical significance in several organs (Table 1). These differences were most dramatic in the spleen where there was a significantly higher burden of parasites, even with multiple-corrections testing (170 versus 16 parasites per 10 high powered fields, $p = 0.0046$, Mann-Whitney test).

When CM phenotype diagnoses were considered, HIV-status was unevenly distributed between classes of CM. Patients with CM1 (defined as having dense sequestration without accompanying pathology) had the highest rate of HIV (57%), with all other groups 20% or less (Table S1). Further, as demonstrated here and in previous studies, CM1 patients had a shorter mean duration from start of illness to death, and a higher mean parasite density (Table S1)⁽³⁾. In all CM categories, HIV-positivity was associated with a higher mean parasite burden in the spleen, although the difference was not statistically significant in groups with few numbers. Spleen parasite burden was however, significantly higher in CM1 HIV-positive cases as compared with CM1 HIV-negatives (57 versus 24 parasites, $p = 0.042$) (Table S2).

Though this study does not encompass the full range of HIV disease (from mild to severe AIDS), we still did have a range of viral loads across individuals (16,460 – 1,620,070 viral copies/mL with a mean of 337,391), as previously published⁽³¹⁾. We found no significant association between HIV viral load and spleen parasitemia, though this may be due to the fact that no patients were in the most severe categories of infection (none with AIDS).

Enrichment of asexual and not sexual stages in the spleens of HIV-positive individuals

This enrichment of parasites in the spleen of HIV-infected patients was confirmed by further detailed studies using stage-specific markers on a subset of these individuals for which high quality tissue and RNA was available. For a subset of cases (5 HIV+, 10 HIV-), we performed immunohistochemistry using both the constitutive marker *Plasmodium lactate dehydrogenase* (pLDH) and the sexual stage marker *Pfs16* on nine organs as previously described. Tissue analyses were conducted on 10 HIV-negative cases (including spleen, brain and bone marrow for all ten cases, and heart, lung, gut, liver, kidney and subcutaneous fat for six cases), as previously published⁽²⁶⁾. These were compared to analyses of 5 HIV-positive cases with all nine organs. By quantifying pLDH-labeled parasites in tissue sections from 100 hpf, we found a significantly higher parasite load in HIV patients in 5 of the 9 organs by Mann-Whitney test (Figure 1A). The spleen was among the most significant associations, with spleens from HIV-positive cases having a significantly higher mean overall parasite burden than those from HIV-negative cases (1835 versus 434.2 parasites, $p = 0.032$, Mann Whitney test). The other organs with significantly higher parasite loads in HIV-positive compared to HIV-negatives were the lung (338.6 versus 35.5 parasites, $p = 0.022$), bone marrow (179.1 versus 61.6 parasites, $p = 0.0233$), liver (129 versus 10 parasites, $p = 0.0135$), and kidney (42.23 versus 2 parasites, $p = 0.0078$). We also quantified the number of Pfs16-labeled sexual stages (which are not typically taken up by macrophages⁽³²⁾) and

found that unlike pLDH, Pfs16-positive cells were not consistently higher in HIV-positive cases, and that for some tissues (brain, bone marrow, gut), the mean number of Pfs16-positive cells was higher in HIV-negative than HIV-positive. However, no statistically significant differences were found in Pfs16 levels between HIV-positive and HIV-negative subjects in any of the organs studied (Figure 1B), suggesting asexual stages are largely responsible for the enrichment of parasites in the tissue of HIV-positive patients.

This was further confirmed by quantitative reverse-transcriptase PCR (qRT-PCR) from a subset of cases (4 HIV+, 5 HIV-), comparing relative expression of asexual schizont stage marker *AMA1* with that of the sexual stage marker *Pfs25* in five organs as previously described⁽²⁶⁾ (Figure 1C–D). The mean expression of Pfs25 was lower in HIV-positive versus HIV-negative cases in the majority of tissues surveyed by qRT-PCR, though these differences were not significant, suggesting equivalent amounts of sexual stages in tissues of HIV-positive versus HIV-negative cases. On the contrary, the mean expression of *AMA1* was higher in HIV-positive versus HIV-negative cases in four out of the five tissues, with the spleen of HIV-positive individuals having a significantly higher expression of the asexual schizont gene *AMA1* as compared with the spleen of HIV-negative individuals (mean fold change of 1.052 versus 0.093, $p = 0.0357$, Mann Whitney test). Altogether, this indicates that the observed enrichment of parasites in the organs, and specifically spleen, of HIV-positive patients is due to an increased load of the asexual stages of the parasite's life cycle.

Dysfunctional phagocytosis in the spleens of HIV-positive individuals

Depigmented Giemsa stained as well as immunohistochemically-labeled spleens showed not only higher burdens of parasites in HIV-infected patients, but also revealed distinct histological differences between the categories. The presence of “free” parasites, i.e. those not found within engulfing macrophages, were commonly observed in the spleen of HIV-positive individuals (Figure 2). Large macrophages containing parasites were more commonly observed in HIV-negative individuals (Figure 2B), while dispersed parasites outside of host cells were observed in HIV-positive cases (Figure 2A) in a standard Giemsa stain. Using immunohistochemistry, we observed clusters of the parasite digestion product hemozoin co-localized within CD163-labeled macrophages in HIV-negative spleens (Figure 2D). In contrast, hemozoin is very clearly localized outside of host cells in HIV-positive spleens (Figure 2C). Polarizing light provided additional evidence of a pattern of scattered hemozoin representing free parasites in HIV-infected patients while abundant pigment-aggregating macrophages were evident in HIV-negative patients (Figure S1). Finally, immunohistochemical labeling of parasites using pLDH shows parasites localized within macrophages in HIV-negative spleens (Figure 2F) while parasites in HIV-positive spleens were observed outside of macrophages (Figure 2E).

Immunohistochemistry labeling for CD8, a marker of macrophages as well as the littoral cell network, demonstrated that parasitized red cells in the spleen are found at the littoral cell borders. This represents the barrier back into the circulation, confirming they are in fact located in the slow circulation network of the spleen (Figure S2). As compared to the spleens in the HIV-negative cases, the histology of the HIV-positive spleens revealed an

enrichment of parasitized red cells that did not appear to be sequestered within the spleen or engulfed by macrophages.

DISCUSSION

In this study, we set out to investigate whether HIV infection was associated with specific histological findings within CM1 and across CM categories. We found that HIV positivity, regardless of cerebral malaria category, was associated with faster progression from illness onset to death, and with higher parasite burdens in the spleen as well as other organs. This observation was recently shown by peripheral blood studies as well⁽³³⁾. The HIV-associated differences in parasite burden pertained specifically to the asexual fraction of the parasites; we noted no significant difference in the burden of gametocytes across these organs. We further investigated whether the increased circulating parasite density in HIV-infected subjects might be related to splenic dysfunction. Across groups, but most strikingly within the CM1 group (the group with the highest rate of HIV), we found evidence of splenic dysfunction, including enrichment of free (unphagocytosed) parasites and, conversely, a decreased numbers of parasite-containing macrophages in HIV-positive cases.

We hypothesized that when the ability of splenic macrophages to phagocytose parasitized red cells is blocked, the splenic filtration of parasitized red cells is overwhelmed, and a high total body parasitemia is achieved rapidly, akin to what is observed in splenectomized individuals^(9, 10). In this study we thus tested whether cases of cerebral malaria in which the spleen's capacity is overwhelmed were associated with a higher parasite burden in the spleen, and body-wide.

Our findings support such a model, in that we observe what appears to be an overwhelmed spleen in CM1-HIV infection (i.e., high burden of parasites in spleen and elsewhere in the body, lack of macrophages phagocytosing in spleens). In this subgroup, we observed a decrease of parasite-containing macrophages, paired with an increase of free unphagocytosed parasites in the spleens of these individuals as compared with CM1 cases that did not have HIV. Though this observation of the host-parasite histology was not found consistently with other clinical CM categories, the increased parasite load in the spleen was striking across all methodologies and range of CM-phenotype patients we examined in this study. In addition, the fact that we observed these differences to be specific to asexual parasites, which are well known to be efficiently targeted by macrophages, is also of great relevance. Since sexual parasites are not efficiently taken up by macrophages, in this sense, they can be seen as a control population of malaria parasites that are presumably unaffected by macrophage-mediated immune clearance^(26, 29). Our data indicate that macrophage dysfunction was associated with high burdens of asexual parasites in HIV-positive patients, an observation that further supports the hypothesis that HIV is associated with macrophage dysfunction, and normal splenic immune clearance of asexual parasites. This may contribute to an accelerated progression toward severe malaria and death. We plan to do a further detailed analysis of the exact quantity, distribution, and immunophenotype of these macrophages in a future study.

From the data we present here, we conclude that HIV infection in children is associated with rapid onset of cerebral malaria, and that this association may be mediated by defects in macrophage phagocytosis which diminish the spleen's ability to clear infection. As malaria endemic areas often overlap with areas in which HIV incidence is high, acceleration of cerebral malaria disease by HIV is of great clinical importance. Similar mechanisms may be occurring in HIV-negative CM1 patients and warrant further study.

Supplementary Material

Refer to Web version on PubMed Central for supplementary material.

Acknowledgments

We would like to thank the parents and families of Malawi for their continued support of this ongoing project as well as the children of Malawi for their participation. We extend very special thanks to the indispensable team in Malawi and our US and UK collaborators that made and continues to make these autopsy tissue and clinical studies possible: George Liomba, Charles Dzamalala, Sam Wassmer, Jacqui Montgomery, Kami Kim, Sarah Hochman, Clarissa Valim, Javier Ogembo, Joyce Fingerroth, Rob Heyderman, Dumizulu Tembo, Jimmy Vareta, Fingani Mphande, Wales Namanya, Johanness Kaliwambe, and Laston James Mbewe.

References

1. Newton CR, Hien TT, White N. Cerebral malaria. *Journal of neurology, neurosurgery, and psychiatry*. 2000; 69:433–41.
2. Taylor TE, Fu WJ, Carr RA, et al. Differentiating the pathologies of cerebral malaria by postmortem parasite counts. *Nature medicine*. 2004; 10:143–5.
3. Milner D Jr, Factor R, Whitten R, et al. Pulmonary pathology in pediatric cerebral malaria. *Human pathology*. 2013; 44:2719–26. [PubMed: 24074535]
4. Safeukui I, Correas JM, Brousse V, et al. Retention of Plasmodium falciparum ring-infected erythrocytes in the slow, open microcirculation of the human spleen. *Blood*. 2008; 112:2520–8. [PubMed: 18579796]
5. Li J, Dao M, Lim CT, Suresh S. Spectrin-level modeling of the cytoskeleton and optical tweezers stretching of the erythrocyte. *Biophysical journal*. 2005; 88:3707–19. [PubMed: 15749778]
6. Engwerda CR, Beattie L, Amante FH. The importance of the spleen in malaria. *Trends in parasitology*. 2005; 21:75–80. [PubMed: 15664530]
7. MacPherson GG, Warrell MJ, White NJ, Looareesuwan S, Warrell DA. Human cerebral malaria. A quantitative ultrastructural analysis of parasitized erythrocyte sequestration. *The American journal of pathology*. 1985; 119:385–401. [PubMed: 3893148]
8. Seydel KB, Milner DA Jr, Kamiza SB, Molyneux ME, Taylor TE. The distribution and intensity of parasite sequestration in comatose Malawian children. *The Journal of infectious diseases*. 2006; 194:208–5. [PubMed: 16779727]
9. Bach O, Baier M, Pullwitt A, et al. Falciparum malaria after splenectomy: a prospective controlled study of 33 previously splenectomized Malawian adults. *Transactions of the Royal Society of Tropical Medicine and Hygiene*. 2005; 99:861–7. [PubMed: 16099487]
10. Buffet PA, Safeukui I, Deplaine G, et al. The pathogenesis of Plasmodium falciparum malaria in humans: insights from splenic physiology. *Blood*. 2011; 117:381–92. [PubMed: 20852127]
11. Subramaniam K, Plank RM, Lin N, et al. Plasmodium falciparum Infection Does Not Affect Human Immunodeficiency Virus Viral Load in Coinfected Rwandan Adults. *Open forum infectious diseases*. 2014; 1:ofu066. [PubMed: 25734136]
12. Kublin JG, Patnaik P, Jere CS, et al. Effect of Plasmodium falciparum malaria on concentration of HIV-1-RNA in the blood of adults in rural Malawi: a prospective cohort study. *Lancet*. 2005; 365:233–40. [PubMed: 15652606]

13. Hoffman IF, Jere CS, Taylor TE, et al. The effect of Plasmodium falciparum malaria on HIV-1 RNA blood plasma concentration. *Aids*. 1999; 13:487–94. [PubMed: 10197377]
14. French N, Nakiyingi J, Lugada E, et al. Increasing rates of malarial fever with deteriorating immune status in HIV-1-infected Ugandan adults. *Aids*. 2001; 15:899–906. [PubMed: 11399962]
15. Ariyoshi K, Schim van der Loeff M, Berry N, Jaffar S, Whittle H. Plasma HIV viral load in relation to season and to Plasmodium falciparum parasitaemia. *Aids*. 1999; 13:1145–6. [PubMed: 10397550]
16. Berg A, Patel S, Aukrust P, et al. Increased severity and mortality in adults co-infected with malaria and HIV in Maputo, Mozambique: a prospective cross-sectional study. *PloS one*. 2014; 9:e88257. [PubMed: 24505451]
17. Flateau C, Le Loup G, Pialoux G. Consequences of HIV infection on malaria and therapeutic implications: a systematic review. *The Lancet infectious diseases*. 2011; 11:541–56. [PubMed: 21700241]
18. Hendriksen IC, Ferro J, Montoya P, et al. Diagnosis, clinical presentation, and in-hospital mortality of severe malaria in HIV-coinfected children and adults in Mozambique. *Clinical infectious diseases : an official publication of the Infectious Diseases Society of America*. 2012; 55:1144–53. [PubMed: 22752514]
19. Sanyaolu AO, Fagbenro-Beyioku AF, Oyibo WA, et al. Malaria and HIV co-infection and their effect on haemoglobin levels from three health-care institutions in Lagos, southwest Nigeria. *African health sciences*. 2013; 13:295–300. [PubMed: 24235927]
20. Keen J, Serghides L, Ayi K, et al. HIV impairs opsonic phagocytic clearance of pregnancy-associated malaria parasites. *PLoS medicine*. 2007; 4:e181. [PubMed: 17535103]
21. Ludlow LE, Zhou J, Tippett E, et al. HIV-1 inhibits phagocytosis and inflammatory cytokine responses of human monocyte-derived macrophages to P. falciparum infected erythrocytes. *PloS one*. 2012; 7:e32102. [PubMed: 22363802]
22. Milner DA, Valim C, Carr RA, et al. A histological method for quantifying Plasmodium falciparum in the brain in fatal paediatric cerebral malaria. *Malar J*. 2013; 12:191. [PubMed: 23758807]
23. MD, JLL, CF, et al. Quantitative Assessment of Multiorgan Tissue Sequestration in Fatal Pediatric Cerebral Malaria. *The Journal of infectious diseases*. 2015
24. Whitten R, Milner DA Jr, Yeh MM, et al. Liver pathology in Malawian children with fatal encephalopathy. *Human pathology*. 2011; 42:1230–9. [PubMed: 21396681]
25. Bancroft, JDGM. *Theory and Practice of Histological Techniques*. 5. London: 2002.
26. Joice R, Nilsson SK, Montgomery J, et al. Plasmodium falciparum transmission stages accumulate in the human bone marrow. *Science translational medicine*. 2014; 6:244re5.
27. Ogembo JG, Milner DA Jr, Mansfield KG, et al. SIRPalpha/CD172a and FHOD1 are unique markers of littoral cells, a recently evolved major cell population of red pulp of human spleen. *Journal of immunology*. 2012; 188:4496–505.
28. Genrich GL, Guarner J, Paddock CD, et al. Fatal malaria infection in travelers: novel immunohistochemical assays for the detection of Plasmodium falciparum in tissues and implications for pathogenesis. *The American journal of tropical medicine and hygiene*. 2007; 76:251–9. [PubMed: 17297032]
29. Aguilar R, Magallon-Tejada A, Achtman AH, et al. Molecular evidence for the localization of Plasmodium falciparum immature gametocytes in bone marrow. *Blood*. 2014; 123:959–66. [PubMed: 24335496]
30. Daily JP, Scandfeld D, Pochet N, et al. Distinct physiological states of Plasmodium falciparum in malaria-infected patients. *Nature*. 2007; 450:1091–5. [PubMed: 18046333]
31. Hochman SE, Madaline TF, Wassmer SC, et al. Fatal Pediatric Cerebral Malaria Is Associated with Intravascular Monocytes and Platelets That Are Increased with HIV Coinfection. *mBio*. 2015; 6:e01390–15. [PubMed: 26396242]
32. Healer J, Graszynski A, Riley E. Phagocytosis does not play a major role in naturally acquired transmission-blocking immunity to Plasmodium falciparum malaria. *Infection and immunity*. 1999; 67:2334–9. [PubMed: 10225892]
33. Rattanapunya S, Kuesap J, Chaijaroenkul W, Rueangweerayut R, Na-Bangchang K. Prevalence of malaria and HIV coinfection and influence of HIV infection on malaria disease severity in

population residing in malaria endemic area along the Thai-Myanmar border. *Acta tropica*. 2015; 145:55–60. [PubMed: 25728746]

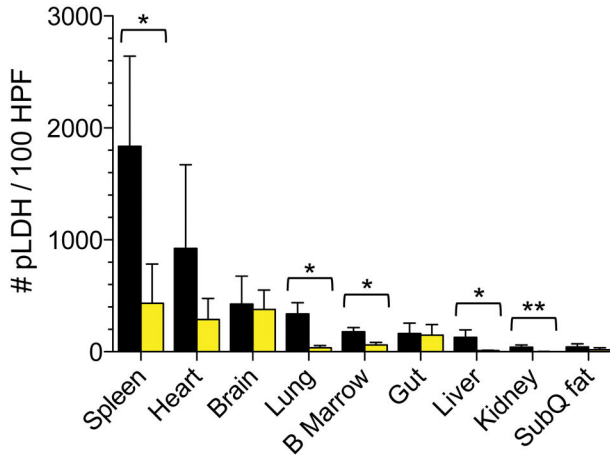
Author Manuscript

Author Manuscript

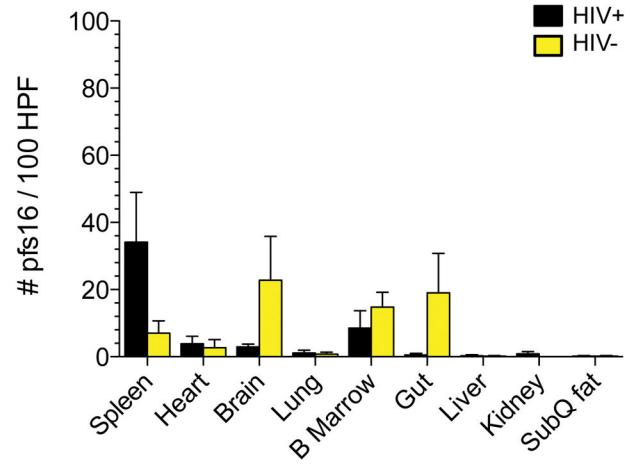
Author Manuscript

Author Manuscript

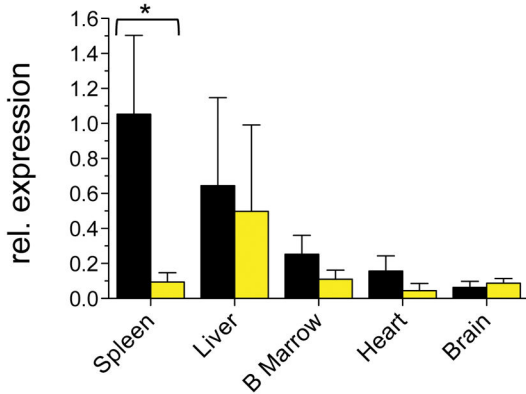
a IHC Quantification of *pLDH* (all parasites)



b IHC Quantification of *Pfs16* (gametocytes)



c qPCR Expn of *PfAMA1* (schizonts)



d qPCR Expn of *Pfs25* (gametocytes)

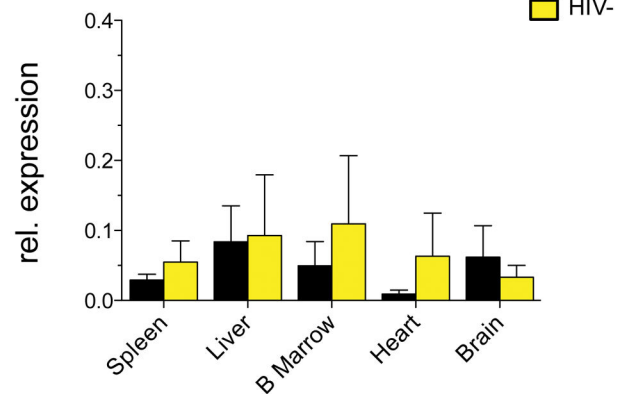


Figure 1. Increased asexual parasite burden observed across tissues in HIV+ cases

Quantities of immunohistochemistry-based (a) *pLDH*-labeled parasites and (b) *Pfs16*-labeled gametocytes quantified in 100 HPF of tissue sections from HIV+ (black bars) and HIV- cases (yellow bars) reveal a significantly higher burden of parasites in the spleen, lung, bone marrow, liver and kidney tissue of HIV+ cases. HIV- positive cases (N=5) include all nine organs, and HIV-negative cases (N=10) include spleen, brain and bone marrow for all ten cases, and heart, lung, gut, liver, kidney and fat for six cases. Relative gene expression, as assessed by qRT-PCR of a schizont marker (*PfAMA1*, c) and a gametocyte marker (*Pfs25*, d), normalized to a constitutively expressed parasite marker *Ubiquitin Conjugating Enzyme (UCE)* of the spleen, liver, bone marrow, heart and brain of 4 HIV+ (black bars) and 3 HIV- cases (yellow bars) reveal a significant enrichment of *P. falciparum* asexual schizont transcripts in the spleens of HIV+ versus HIV- cases. Statistical analyses were done using Mann-Whitney test. Brackets denote comparisons in which there is a significant difference between HIV+ and HIV- marker level. Asterisks denote the p-value level (*, $p < 0.05$ and **, $p < 0.01$).

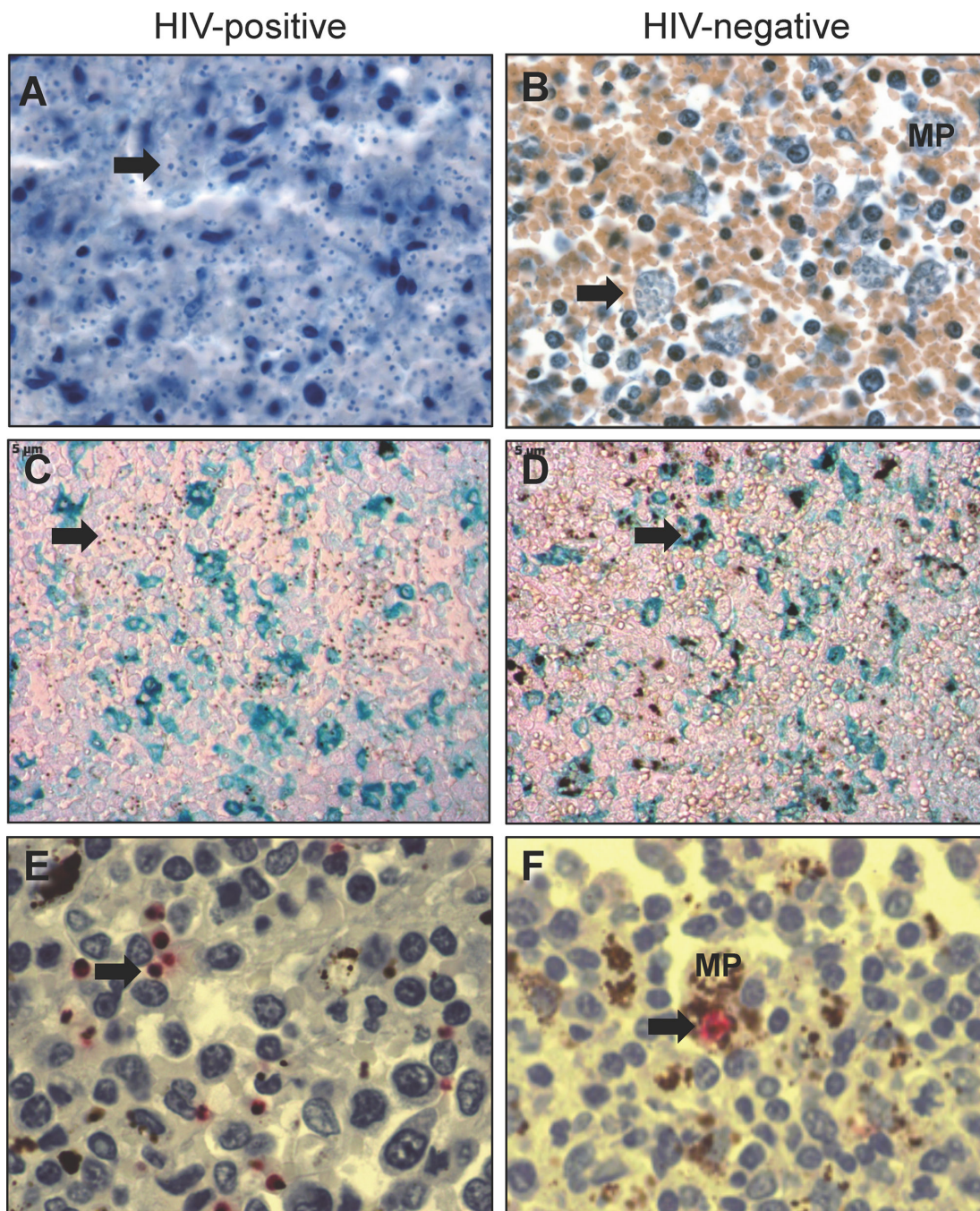


Figure 2. Histological differences in parasites in the spleen of HIV-positive versus HIV-negative patients

Image panels of histological sections from spleens of HIV-positive (A, C, E) and HIV-negative (B, D, F) cases. H&E stained de-pigmented sections (400X) reveal a large number of free parasites, labeled in blue with hematoxylin (arrow), in the HIV+ spleen (A), compared with a large number of phagocytosed parasites (arrow) in the HIV- spleen (B) [color differences in red cells represents variability in tissue processing and staining]. Immunohistochemistry with CD163 labeling (macrophages, blue) sections (shown at 50X) also reveal free parasites (arrow) in the HIV+ spleen, as seen by small distributed hemozoin

pigment (C) compared with the HIV– spleen (D) showing a large amount of clumped hemozoin phagocytosed by macrophages (shown in turquoise, arrow).

Immunohistochemistry with pLDH labeling (parasites, red) and hematoxylin counterstain revealing large trophozoite-stage parasites distributed across the spleen (arrow) in HIV+ case (E), compared with a phagocytosed parasite (arrow) in a macrophage in the HIV– case (F). In panels B and F where macrophages were not labeled with a specific marker, macrophages were identified morphologically and labeled “MP”.

Table 1

Summary of clinical parameters and tissue histology parasite counts by HIV status for patients with histologically diagnosed CM

Histologically Confirmed Cerebral Malaria			
	HIV +	HIV –	P-value
Demographics & History			
Age (months)	79 [37 – 106]	26 [20 – 43]	0.0023
Gender (% male)	47%	51%	0.5000
Onset of Symptoms to Death	50 [29 – 57]	78 [52 – 106]	0.0084
Laboratory			
Parasitemia (pX10³/uL)	202 [29 – 325]	74 [8 – 424]	0.6350
Hematocrit (%)	20 [18 – 26]	20 [15 – 26]	0.7006
Lactate (mmol/L)	11.1 [9 – 12.3]	11.9 [5.9 – 15.1]	0.4638
White Cell Count (cellsX10³/uL)	13.6 [11.9 – 14.7]	11.2 [8.8 – 18.4]	0.6334
Platelets (cells × 10³/uL)	77 [36 – 144]	50 [26 – 83]	0.0592
Tissue Histology Counts[*]			P-value^{**}
Brain (% vessels parasitized)	82%	72%	0.0907
Brain (pp/100 capillaries)^{***}	371 [169 – 473]	219 [92 – 319]	0.1289
Lung (pp/10 hpf)	26 [14 – 115]	30 [19 – 75]	0.7917
Heart (pp/10 hpf)	85 [7 – 128]	12 [5 – 34]	0.0110
Stomach (pp/10 hpf)	116 [16 – 567]	51 [13 – 120]	0.3389
Jejunum (pp/10 hpf)	188 [53 – 1983]	87 [31 – 454]	0.2428
Ileum (pp/10 hpf)	110 [3 – 276]	47 [13 – 86]	0.3609
Colon(pp/10 hpf)	215 [51 – 695]	53 [14 – 405]	0.1904
Spleen (pp/10 hpf)	170 [70 – 222]	16 [4 – 85]	0.0046
Skin (pp/10 hpf)	105 [0 – 1185]	94 [30 – 144]	0.9264

* All continuous data shown as Median [interquartile range] with Mann-Whitney statistical tests

** Mann-Whitney with Bonferroni correction for multiple testing (11 tests)

*** Tissue histology counts are in pigmented (i.e. late trophozoite/schizont) parasites (pp)